Since January 2020 Elsevier has created a COVID-19 resource centre with free information in English and Mandarin on the novel coronavirus COVID-19. The COVID-19 resource centre is hosted on Elsevier Connect, the company's public news and information website.

Biosensors and Bioelectronics 100 (2018) 312–325

Contents lists available at ScienceDirect

Biosensors and Bioelectronics

journal homepage: www.elsevier.com/locate/bios

Recent advances in nanowires-based field-effect transistors for biological sensor applications

Rafiq Ahmad*, Tahmineh Mahmoudi, Min-Sang Ahn, Yoon-Bong Hahn*

School of Semiconductor and Chemical Engineering, Nanomaterials Processing Research Center, Chonbuk National University, 567 Baekjedaero, Deokjin-gu, Jeonju-si, Jeollabuk-do 54896, Republic of Korea

ARTICLE INFO

Keywords:
Nanowires
Field-effect transistors
Biological sensors
Biomolecules

ABSTRACT

Nanowires (NWs)-based field-effect transistors (FETs) have attracted considerable interest to develop innovative biosensors using NWs of different materials (i.e. semiconductors, polymers, etc.). NWs-based FETs provide significant advantages over the other bulk or non-NWs nanomaterials-based FETs. As the building blocks for FET-based biosensors, one-dimensional NWs offer excellent surface-to-volume ratio and are more suitable and sensitive for sensing applications. During the past decade, FET-based biosensors are smartly designed and used due to their great specificity, sensitivity, and high selectivity. Additionally, they have the advantage of low weight, low cost of mass production, small size and compatible with commercial planar processes for large-scale circuitry. In this respect, we summarize the recent advances of NWs-based FET biosensors for different biomolecule detection i.e. glucose, cholesterol, uric acid, urea, hormone, proteins, nucleotide, biomarkers, etc. A comparative sensing performance, present challenges, and future prospects of NWs-based FET biosensors are discussed in detail.

1. Introduction

The rapid development of nanoscience and nanotechnology has created an overwhelming stream of opportunities to manufacture nano-sized systems that perform specific electrical, mechanical, biological, chemical, or computing tasks (Huang et al., 2011b; Monopoli et al., 2012). It is well known, when the materials size are brought to nanoscale sizes they suddenly display very different properties compared to their original properties as a bulky material (Vigneshvar et al., 2016). A variety of nanomaterials has been synthesized using different preparation methods (Yang et al., 2015; Sadeghian et al., 2017; Ahmad et al., 2017a, 2017b, 2017c; Ashley et al., 2017; Luong and Vashist, 2017; Shrestha et al., 2017). Among diverse nanomaterials architectures, NWs are highly functional structures and offer unique properties due to their one dimensionalities. Especially, the electrical conductivity through NWs is greatly affected by the biological/chemical species adsorbed on their surface. Hence, NWs are effectively used to develop nanoscale devices with enhanced sensing performances.

NWs have been used for the integration/immobilization on biosensing devices for clinical, environmental, and industrial applications, which generates novel interfaces that offer improved sensitivity and efficiency to target analytes. Bioanalysis in general and biosensor fields in particular are showing special interest in NWs due to rapid response, small size, and high sensitivity and portability. Moreover, newer NWs with particularly impressive, robust and economically feasible platforms may provide high current amplification and sustain an enhanced signal-to-noise ratio among all the detection methodologies owing to their excellent sensitivity, label-free, real-time response for bio- and chemical molecule detection (Turner, 2013; Citartan et al., 2013; Sang et al., 2015). Other nanomaterials (bulk or non-NWs) nanostructures are also used for the fabrication of FET-based sensing devices. However, such devices made of bulk or non-NWs materials offer poor sensitivity due to the high dimensionality and lower surface-to-volume ratio.

The FET-based biosensors are advantageous over other methods due to the accumulation of charge on the nanomaterials channel between source-drain (S-D) electrodes, which gets affected by external fields and allow rapid analysis of different analytes with great specificity, sensitivity, and high selectivity (Han et al., 2017; Majd et al., 2017; Kaisti, 2017). Recently, FET-based biosensing devices were reported with high sensitivity and easy fabrication process, compared to other biosensing devices (Chen et al., 2011b; Rubtsova et al., 2017; Arya et al., 2015; Huang et al., 2015; Zheng et al., 2015; Zhang et al., 2016; Piccinini

Abbreviations: IGZO, Indium gallium ZnO; CMOS, Complementary metal-oxide semiconductor; PAC, Polymer-like amorphous carbon; AFP, Anti-α-feptoprotein; PSA, Prostate specific antigen; cTnT, Cardiac troponin T; CEA, Carcinoembryonic antigen; PNA, Peptide nucleic acid; APTES, 3-aminopropyltriethoxysilane; BSA, Bovine serum albumin; ALD, Atomic layer deposition; PEDOT, Poly(ethylene dioxythiophene); PSMA, Prostate-specific membrane antigen; AMPs, Antibody mimic proteins

* Corresponding authors.
E-mail addresses: ahmadrafiq38@gmail.com (R. Ahmad), ybhahn@chonbuk.ac.kr (Y.-B. Hahn).

http://dx.doi.org/10.1016/j.bios.2017.09.024
Received 29 July 2017; Received in revised form 8 September 2017; Accepted 14 September 2017
Available online 18 September 2017
0956-5663/

et al., 2017; Jin et al., 2015; Lee et al., 2015b; Tran et al., 2016; Mao et al., 2016; Kim et al., 2016; Minami et al., 2016; Tan et al., 2015; Park et al., 2016; Puchnin et al., 2017). Additionally, FET-based biosensing devices have the advantage of low-weight, low-cost of mass production, small size and compatible with commercial planar processes for large-scale circuitry. During biological fragments analysis, these biosensing devices directly concert the biological actions into electronic signals, which can be the shortest route of detection. Therefore, development of new nanostructured materials for FET-based biosensor fabrication drew more attentions. In this context, this review summarizes the recent advances of NWs-based FET biosensors for different biomolecule detection. Utilization of various materials NW, comparative sensing performance, limitations, present challenges, and future prospects of NWs-based FET biosensors are also discussed.

2. FET-based biosensor

Since the development of first FET in 1970, there has been the major drive to utilize FET-based biosensor devices for different analytes detection (Bergveld, 1970; Balasubramanian, 2010; Cella et al., 2010; Artiles et al., 2011). In these biosensors, current flows along a semiconductor path (the channel) that is connected to two electrodes, S-D. When charged molecules exist on the surface of the FET biosensors, the channel conductance between S-D can be controlled by a third (gate) electrode that is capacitively coupled through a thin dielectric layer (Liu and Guo, 2012; Shoorideh and Chui, 2014). In such devices for insulation, an oxide is used as a gate dielectric, such as silicon dioxide (SiO_2) (Scheme 1a). It also contains a p-type silicon substrate (bulk). Where the negative gate potential leads to the accumulation of holes (majority charge carriers), resulting in an increase of the channel conductance, while the positive gate potential leads to the depletion of holes and hence decrease the conductance. The adsorption of molecules on the surface of the semiconducting channel either changes its local surface potential or directly dopes the channel, resulting in the change of FET conductance. This makes the FET a promising sensing device with easily adaptable configuration, enhanced sensitivity and real-time capability. Additionally, the nonspecific absorption problem is solved using smart chemistry to prevent the fouling of the surface when device is exposed to complex media i.e. human serum/blood (Cheran et al., 2014).

However, in solution-gated FET biosensors, the analytes are detected in an aqueous environment (Scheme 1b). From the scheme, the semiconducting NWs channels are immersed in a flow or sensing chamber, which is used to confine the solution. In such FET biosensors, the source and electrodes are insulated to prevent current leakage from ionic conduction using insulators i.e. poly(methyl methacrylate), poly (dimethylsiloxane)/silicone rubber, SiO_2 thin film, SU8 passivation, and silicone rubber (Yang and Zhang, 2014; Huang et al., 2010, 2011a; Kergoat et al., 2012; Chen et al., 2013; Feigel et al., 2011; Sudibya et al., 2011). The gate electrode (Ag/AgCl or Pt) is immersed in the solution. Due to the small size of devices, use of a conventional reference electrode limits seriously. Therefore, the development of a miniature reference electrode is necessary. At the channel/solution interface, the gate potential is applied through thin electric double layer capacitance. The sensing performance of FET biosensors depends on the variety and thickness of the gate insulators. The ionic strength of solution determines the double-layer thickness (or Debye length), which is typically within 1 nm. Maehashi et al. (2013) have demonstrated a graphene-based FET for the detection of K/Na ions in solution. In this report, the solution-gated FET was over two orders of magnitude more sensitive than the typical back-gate FET.

3. NWs-based FET biosensor

Wide range of nanomaterials has been used as channel materials to fabricate metal-oxide semiconductor FET, ion-selective FET, and NWs-based FET biosensors, where prepared channel remain in direct contact with the environment, and this gives better control over the surface charge (Shavanova et al., 2016; Wang et al., 2014; Jiang, 2011; Sarkar et al., 2014; Liu and Guo, 2012). Thus far, considerable efforts have been made to develop better FET architecture by incorporating different metals (Ag, Pt, Au, and Cu), semiconductor (ZnO, SnO_2, Si, GaN, TiO_2, In_2O_3, InP, etc.), and polymer NWs to study biomolecular interactions and overcome the physical limitations of FET technology. These NWs fabrication processes are mainly categorized into bottom-up and top-down techniques (Hobbs et al., 2012; Namdari et al., 2016). Scheme 2 is showing the schematic representation of bottom-up and top-down technologies have been demonstrated using different methods. The top-down approach is important as it can accurately align and control identical precise directions of NWs. However, it cannot achieve as good down-scaling as bottom-up approach. Importantly, NWs-based FET biosensors have been reported to tackle multiple limitations, and thus, they are most effectively used for FET-based biosensors fabrication. We reviewed semiconductor and polymer NWs-based FETs in the following sections and presented a brief comparison of semiconductor and polymer NWs-based FETs biosensors in Table 1.

3.1. Semiconductor NWs-based FET biosensor

3.1.1. Zinc oxide NWs-based FET biosensor

Zinc oxide (ZnO) is one of the most exciting materials for FET-based biosensors fabrication due to its versatile properties (Hahn, 2011; Shen et al., 2016; Ahmad et al., 2015; Drobek et al., 2016; Sinha et al., 2016; Asif et al., 2009; Wang et al., 2016; Ye et al., 2016). The high

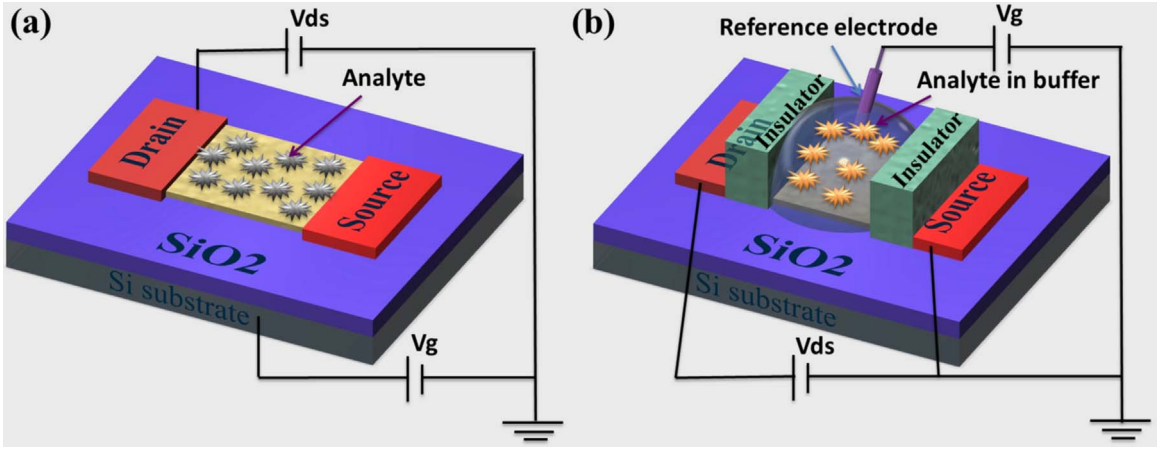

Scheme 1. Schematic illustration of (a) a typical back-gated and (b) solution-gated FET biosensors used in chemical and biological sensing applications.

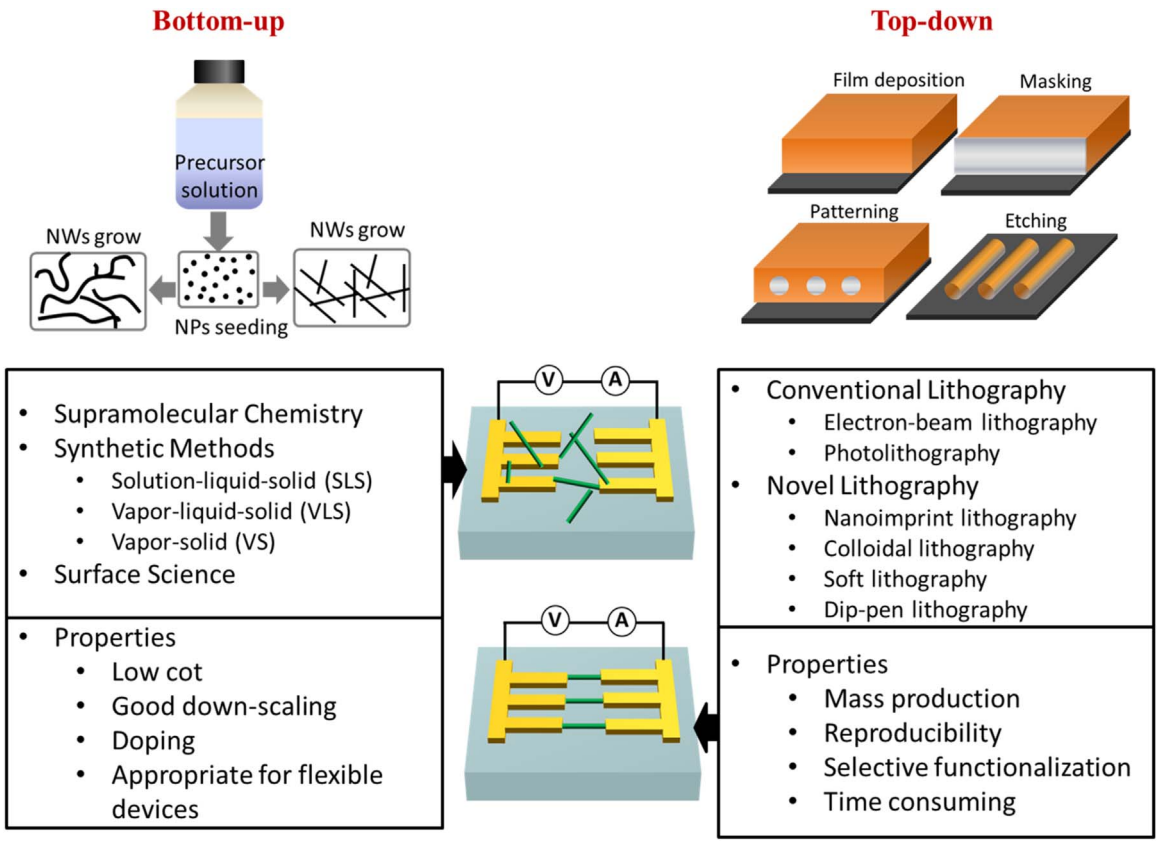

Scheme 2. NWs assembly on device substrates using bottom-up and top-down fabrication approaches.

isoelectronic point (IEP; 9.5) of ZnO enables high loading of low IEP enzymes/proteins (Ahmad et al., 2013). Recently, ZnO NWs-based FET biosensors for glucose detection were reported with enhanced sensing performances. Importantly, in an aqueous environment the fabricated glucose sensing device sensed glucose in the concentration range of 0.1–100 mM with high sensitivity, which matches the physiological concentration of glucose (1–20 mM) in humans (Heller and Feldman, 2008). Yu et al. (2013) demonstrated the fabrication of a self-powered, piezotronic effect enhanced glucose sensor based on metal-semiconductor-metal structured single ZnO NW device. The results showed that piezotronic effect significantly raises the sensitivity as well as improve the sensing resolution of ZnO NW-based glucose sensors and provides a possible way to build up a self-powered glucose monitoring system.

For further advancement in glucose sensing, Du et al. (2016) reported bottom-gated indium gallium ZnO (IGZO) FET for noninvasive continuous glucose monitoring and device integration into contact lenses. Fig. 1 shows the optical image (a) and schematic of the device (b) along with transfer characteristics of glucose oxidase (GOx) functionalized IGZO FET after exposure to varying concentrations of glucose (c). They functionalized the back channel of IGZO-FETs with aminosilane groups that were cross-linked to GOx and have demonstrated that these devices have high sensitivity to changes in glucose concentrations. Glucose sensing occurs through the decrease in pH during glucose oxidation, which modulates the positive charge of the aminosilane groups attached to the IGZO surface (d). The change in charge affects the number of acceptor-like surface states, which can deplete electron density in the n-type IGZO semiconductor. Increasing glucose concentrations leads to an increase in acceptor states and a decrease in S-D conductance due to a positive shift in the turn-on voltage. This study advances the development of oxide-based FETs for applications to glucose biosensors with the potential to integrate fully transparent

Table 1
Brief comparison of semiconductor and polymer NWs-based FET biosensors.

Biosensor device	Merits	Demerits
Semiconductor NWs-based FET	Fabricated relatively cheaply in parallel with traditional microfabrication techniques.	Needs well-defined NW structures with controlled atomic compositions and heterojunctions to fabricate highly reproducible devices.
	Being a sensitive, semiconductor transducers offer electrical transduction in terms of realization of simple, portable and inexpensive devices.	Small size of device poses challenges when integrated in microfluidic systems.
	Utilization of biocompatible NWs with potential to easily attach various receptor molecules.	Difficult to avoid nonspecific interactions during application in whole blood/serum
Polymer NWs-based FET	Simple fabrication techniques and tunable properties (electrical, mechanical and optical).	Lack of incompatibility with traditional microfabrication techniques.
	Facile functionalization routes and biocompatibility of polymer NWs make them attractive alternative over other nanomaterials based FETs.	It demands precise control over possible thermal damages and unstable contact of polymer NWs with metal electrodes in device architecture.
	An array of polymer NWs with multi-functionality based FETs have potential for the detection of multiple analytes.	Mechanical/thermal stability and durability of polymers limit the utility of polymer NWs-based FET biosensors.

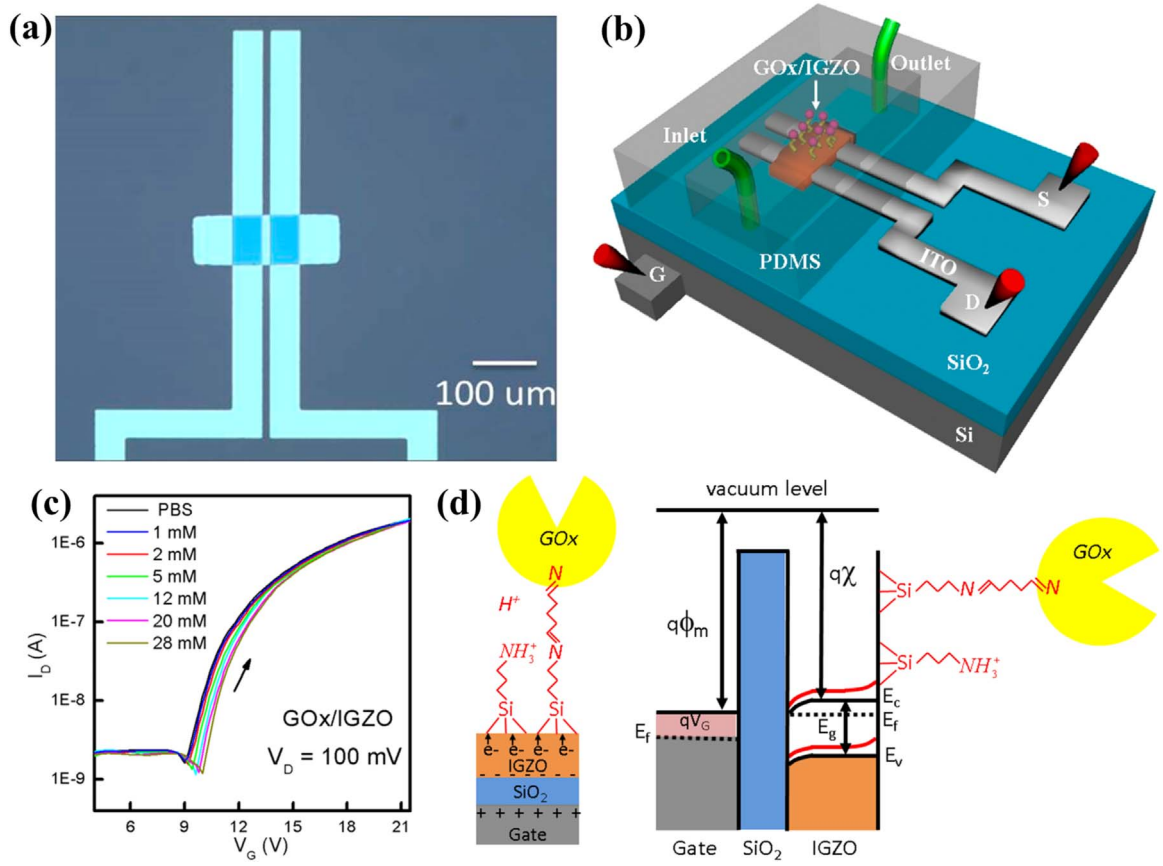

Fig. 1. (a) Optical images of IGZO-TFT device; (b) Schematic illustration of experimental apparatus for IGZO-FET sensor; (c) Transfer characteristics of GOx functionalized IGZO-FET after exposure to different concentrations of glucose; and (d) Schematic diagram showing the role of positively charged aminosilane groups as an electron acceptor and the impact of positively charged aminosilane groups on band bending at IGZO surface. Images reprinted from (Du et al., 2016).

sensors into contact lenses.

NW-based sensing devices have been also used due to monitor uric acid and urea concentrations in blood samples to evaluate a type of arthritis (gout) and kidney disease (Rees et al., 2014; Weintraub et al., 2015). For uric acid detection, Liu et al. (2013) fabricated single ZnO NW-based FET biosensor and detected uric acid in vitro (Fig. 2). The cross-linking method was used to immobilize uricase on ZnO NWs and device characteristics were measured, which showed high on/off ratio and very low transconductance of ~4.6 $\times 10^6$ and ~8.2 nS, respectively. While increasing uric acid concentration, a rapid increase in device conductance was recorded at room temperature in an ambient environment. The response time turned out to be in the order of a millisecond, which is relatively short compared to other diagnostic technologies. Also, the sensor was more sensitive at low uric acid concentrations than at high concentrations. High selectivity, low detection limit, and cost-effective approach of the device can be further exploited by expanding into arrays for portable, reliable and real-time detection of analytes.

In spite a lot of uses of ZnO NWs for chemical and biological sensing applications, they show some drawbacks like chemical instability in the liquid solution that may lead to decrease in sensing performance of biosensors. To protect NWs from the harsh environment and enhance electrical conductance, some groups have used effective surface modification platforms (Keem et al., 2007; Ra et al., 2012). Also, the charge transport in single NW strongly depends on its surface environmental conditions and can be explained by the formation of depletion layer at the surface by various surface states present on it. As known, that the ZnO NWs contains a lot of surface oxygen sites due to the very large surface-to-volume ratio. According to this phenomenon, the surface electron depletes from the surface of the ZnO NW and hence decreases the channel conductivity. Verma et al. (2008) reported an ultraviolet irradiation treatment method at high temperature and vacuum. Where ultraviolet light stimulated oxygen desorption from the active channel and improves the device performance (~17 times) of ZnO NW-FETs. The nondestructive surface cleaning removes these absorbed surface states from the NW and the current values increase up to ~7 μA from ~0.4 μA at a bias voltage of 3 V. Recently, Choi et al. (2010) also used physical method to change the conductance of ZnO NWs surface through modification that also enhances the enzyme immobilization efficiency. The fabricated FET-based biosensor-utilizing surface modified ZnO NWs were further characterized for streptavidin detection. The ZnO NW biosensors easily detect streptavidin binding down to a concentration of 2.5 nM in an enhancement mode with a higher sensitivity compared to other NW-based biosensors.

For further advancement, Ra et al. (2012) demonstrated a robust and multifunctional nanosheath based on nonthermal plasma technology, which can overcome the problem of the chemical instability of the core ZnO NWs in a solution environment and make it possible for them to serve as pH sensors and biosensors. A polymer-like amorphous carbon (PAC) was deposited on ZnO NWs during nonthermal plasma technology-based chemical modifications on the surface, which were subsequently used for amino group's formation for the effective immobilization of biomolecules. The additional advantage of this approach allows controlling the thickness of the PAC shell on the ZnO NWs without any significant changes in the electrical properties of the ZnO NWs (Ra et al., 2009). Further, the potential biosensor applications showed that the amino functionalized ZnO/PAC NW FETs can be directly employed for the real-time, label-free detection of anti-α-fepto-protein (AFP). The anti-AFP modified NW FET was successfully applied to the real-time, label-free detection of cancer biomarkers in human

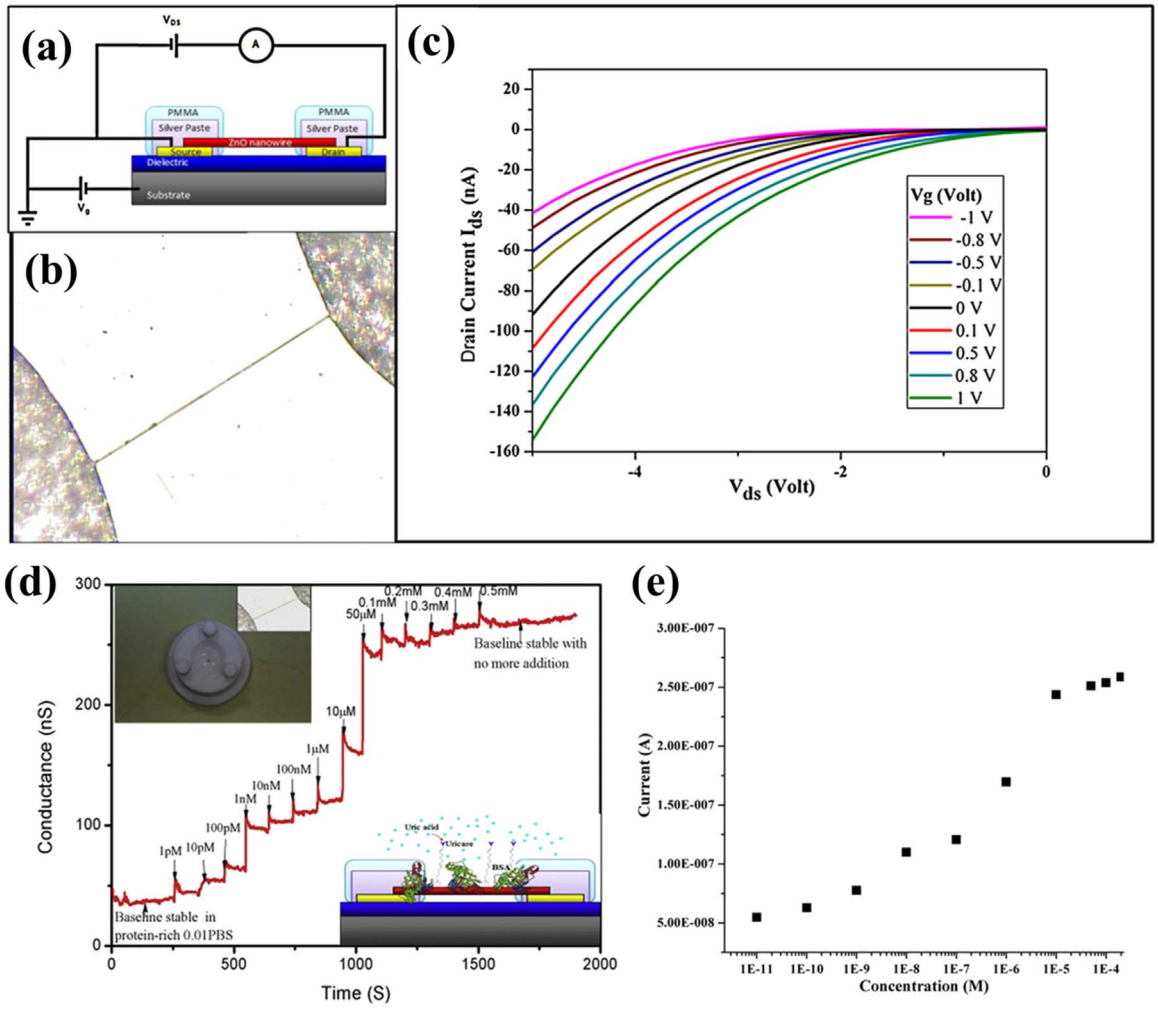

Fig. 2. (a) Schematic of single ultra-long ZnO NW FET biosensor system; (b) Optical image of biosensor; (c) Device characteristics under varying gate voltage at fixed S-D voltage of −1 V; (d) Real time measurement with addition of uric acid in the buffer solution; and (e) Calibrated plot. Upper and lower inset in d are showing the homemade reaction cell with optical image of Ag paste immobilized ultra-long ZnO NW and device configuration, respectively. Images reprinted from (Liu et al., 2013).

serum of a liver carcinoma patient. In particular, this study can be directly extended to high-performance biosensor applications with higher sensitivity and selectivity, since the PAC shell can be easily functionalized for the purpose of covalent binding and steric stabilization.

3.1.2. Silicon NWs-based FET biosensor

Silicon NW (SiNW) has emerged as a promising sensing material and attracted remarkable attention of researchers due to their high surface-to-volume ratios, biocompatibility, unique tunable electrical, optoelectronic and thermal properties (Rashid et al., 2013; Zhang and Ning, 2012; Chen et al., 2011b). These properties greatly enhance the sensing abilities i.e. selectivity and sensitivity, real-time response, and label-free detection capabilities; especially the detection limit can be measured up to femtomolar (fM) concentrations with high sensitivity. Additionally, the small dimension (~1–100 nm) makes them more comparable and compatible to the dimensional scale of biological and chemical species (Nair and Alam, 2007). In FET-based devices, SiNWs with the smallest dimension resulted in fast electron transfer due to direct charge accumulation in NWs that leads to ultrasensitive and selective detection of various analytes.

NWs-based FET biosensors fabricated using top-down lithography has offered greater accuracy, uniformity, and patterning flexibility for device fabrication. Protein detection and investigation in various biological samples such as blood, serum, urine, and saliva is the center to disease diagnosis and treatment. Regonda et al. (2013) proposed to use multiple-nanochannel/nano-grating (NG) as sensing element. They fabricated Si NGs-FETs with highly uniform performance using a complementary metal-oxide semiconductor (CMOS) process on low p-doped silicon-on-insulator wafers (Fig. 3). The use of a Si nano-grating design significantly reduces the device-to-device variation due to reduced discrete doping effects. They detected insulin in the concentration range of 10 fM to 0.1 nM. With these improved devices, selective detection of insulin-analog in both buffer and diluted human serum with LOD down to 10 fM was achieved repeatedly. In another report, Puppo et al. (2014) used single NW-based FET to detected bioanalytes in exogenously added rabbit antigen (5–200 fM) in a human breast tumor extract (a much more complex environment). They detected pathogenic factors at very low concentrations (fM) in PBS in the presence of 100,000 mass excess of the nonspecific tumor protein, indicating that the biosensor is excessively resistant to noise.

Cui et al. (2001) used bottom-up approach to fabricate SiNW-FET for highly sensitive and selective real-time detection of proteins. Due to irreversible biotin-streptavidin binding interaction precludes real-time monitoring of streptavidin down to at least picomolar concentration range. Further in recent reports by Stern et al. (2007a), (2007b), the streptavidin detection limit was improved to fM concentration using top-down fabrication methods. Other important analytes i.e. influenza A virus, prostate specific antigen (PSA), dopamine, carbohydrate antigen-15.3 (CA-15.3), cardiac troponin T (cTnT), creatine kinase, carcinoembryonic antigen (CEA), mucin-1, thyroid-stimulating hormone,

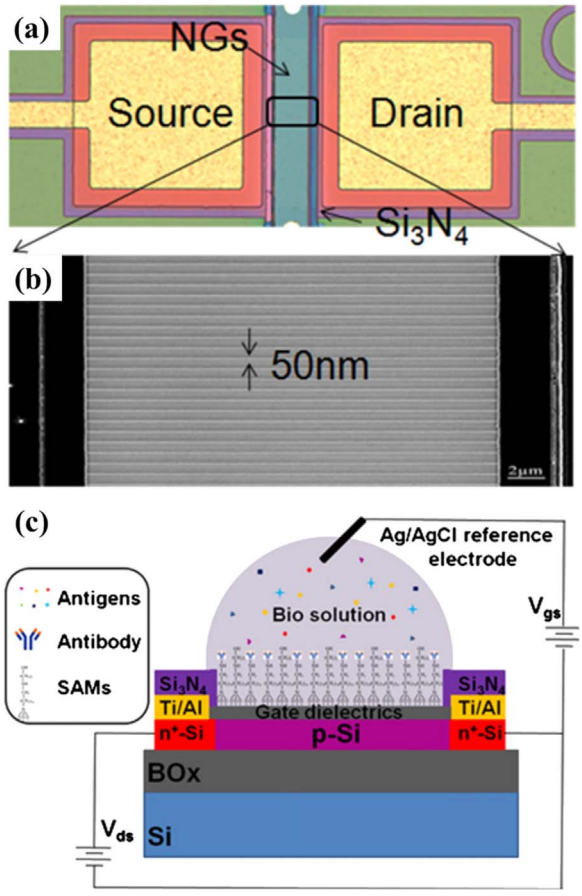

Fig. 3. (a) Optical image of NG-FETs with 100 nanochannels with (b) SEM zoom-in view of nanochannels connecting highly doped S-D pads. (c) Cross-sectional illustration of chemically constructed SiNG FET biosensor. Images reprinted from (Regonda et al., 2013).

troponin I, endoplasmic reticulum, RT-PCR product of dengue serotype 2, and microRNA have been detected using different SiNW-FET devices (Table 2).

In contrast to other analyte detection, DNA detection has been widely researched (Table 2) with peptide nucleic acid (PNA)-DNA and DNA-DNA hybridization methods. In SiNW-FET based biosensors, the sensing mechanism by SiNWs can be understood in terms of the change in charge density which induces a change in the electric field at the SiNW surface after hybridization. As a consequence of the field-effect-based sensing mechanism, the distance of the DNA (charge layer) to the SiNW surface plays a key role in the detection sensitivity. Zhang et al. (2008a, 2008b) have used a top-down approach to fabricated highly sensitive SiNW-FET based biosensors after immobilizing the PNA, which was capable of recognizing the label-free complementary target DNA down to 10 fM. In another approach, Hahm and Lieber (2004) fabricated SiNWs-based devices by the bottom-up method to detect single-stranded (ss) DNA. In this device, PNAs were used as the receptor because the uncharged PNA molecules have greater affinity and stability with corresponding DNA recognition sequences at low ionic strength.

Bunimovich et al. (2006) demonstrated the quantitative, real-time detection of ss-oligonucleotides with SiNWs. The superlattice NW pattern transfer method was used for NW array fabrication and 2 mm long array of 400 SiNWs, each of 20 nm width and patterned at 35-nm pitch were produced (Fig. 4). The electronic measurements showed that a single-stranded complementary oligonucleotide significantly changed the conductance of a group of 20-nm-diameter SiNWs in 0.165 M solution by hybridizing to a primary DNA strand that has been electrostatically adsorbed onto an amine-terminated organic monolayer atop the NWs. This intimate contact of the primary strand with the amine groups of the NW surface brings the binding event close enough to the NW to be electronically detected. In addition, within a 0.165 M ionic strength solution the DNA hybridization was more efficient. Li et al. (2004) reported SiNWs-based highly sensitive and sequence-specific DNA FET device with ss-probe DNA molecules covalently immobilized on the NW surface. Label-free complementary (target) ss-DNA in sample solutions was recognized when the target DNA was hybridized with the probe DNA attached on the SiNW surfaces, producing a change in the conductance of the SiNWs. For a 12-mer oligonucleotide probe, 25 pM of target DNA in solution was detected easily (signal/noise ratio > 6), whereas 12-mers with one base mismatch didnot produce a signal above the background noise. In a similar report, Li et al. (2005) explained the width dependence of the SiNW conductance and provided understanding to improve the sensor performance.

Recently, Nuzaihan et al. (2016) fabricated SiNWs-based FET by direct-write electron beam lithography and successfully detected DNA molecules in a microfluidic environment. The fabricated SiNWs-based FET showed good electrical characteristics after surface modification, DNA immobilization, and DNA hybridization. This approach offers good specificity and sensitivity, with a LOD of 10 fM for target DNA. The current change rate of SiNW-FETs can be exponentially enhanced in the subthreshold regime by both analyses of FET's theory model and electrical characteristics. Pengfei et al. (2013) showed that on the basis of back-gate controlled sensors detection sensitivity for DNA and pH value improves in the subthreshold regime, which shows that optimization of SiNW-FET operating conditions, can provide significant improvement for the limits of SiNW-FET nanosensor and making it possible for higher-accuracy chemical and biological molecules detection. Adam and Hashim (2014) further improved the detection limit with novel liquid gate control for detection of specific ss-DNA molecules.

Ryu et al. (2010) proposed a new method to fabricate SiNW-based biosensor devices after embedding Au nanoparticles (NPs) on SiNW to enhance the sensitivity for label-free DNA detection. Silicon-on-insulator substrate with a top silicon thickness of 110 nm was utilized to fix and connect SiNW both ends to the large pad area in order to provide a measurable contact size. Then, the Au NPs were embedded on the one-dimensional SiNW by sputtering. Schematic and image of device are shown in Fig. 5. The complementary target oligonucleotide, breast cancer DNA with 1 pM, was sensed. In addition, LOD can be improved by reducing the SiNW doping concentration. This emerging architecture combined spherical Au NPs on SiNW has high potential as a label-free biosensor due to its facile fabrication process, high thermal stability, immobilization efficiency with a thiol-group in a self-assembled monolayer, and improved sensitivity. Pham et al. (2011) fabricated SiNW-FET device using deposition and etching under angle (DEA) technique, then used to build up the complete SiNW-based biosensor. The fabricated biosensor detected DNA of genetically modified maize with concentrations down to ~200 pM.

Gao et al. (2011) have given a pioneering and creative study addressing how the fundamental factors (SiNW size, Debye screening, surface chemistry, and charge layer distance from SiNW surface) of the device affect their sensitivity and concluded that detection in the subthreshold regime of NW FET has improved the conductance response and better detection limit (Gao et al., 2012). Under optimal factors, the SiNW-FET nanosensor revealed ultra-high sensitivity for rapid and reliable detection of target DNA with a detection limit of 0.1 fM and high specificity for single-nucleotide polymorphism discrimination, which was 10 times better than their previous report (Gao et al., 2011). Gao et al. (2010) using the bio-recognition layer entrapment method in the gated region of FET demonstrated that the sensitivity of NW-FET biosensor could be rapidly enhanced in the sub-threshold regime because the gating effect of bound molecules on a surface is more effective for reduced charge carriers in NWs.

Table 2
Analytical performance of SiNW based FET biosensors.

Device specification	Fabrication	Mechanism	Application	Detection Limit	Ref.
p-type SiNW; diameter: 20 nm	Bottom-up	Biotin-avidin binding	Streptavidin	10 p.M.	Cui et al. (2001)
p-type SiNW; diameter: 20 nm	Bottom-up	Antibody-virus interaction	Influenza A virus	Single virus	Patolsky et al. (2004)
n-type SiNW, p-type SiNW; diameter: 20 nm	Bottom-up	Antibody-antigen interaction	PSA, CEA, Mucin-1	PSA: 2 fM, CEA: 0.55 fM, Mucin-1: 0.49 fM	Zheng et al. (2005)
p-type SiNW; diameter: 30–60 nm	Bottom-up	Protein-protein interaction	Troponin I	7 nM	Lin et al. (2010)
p-type SiNW; diameter: 20 nm	Bottom-up	PNA-DNA hybridization	DNA	10 fM	Hahm and Lieber (2004)
p-type multi-SiNW; width: 50 nm, thickness: 30 nm, length: 20 μm	Top-down	Antibody-antigen interaction	Insulin	10 fM	Regonda et al. (2013)
p-type single-SiNW	Top-down	Antibody-antigen interaction	Antigen	5 fM	Puppo et al. (2014)
n-type SiNW, p-type SiNW; thickness: 40 nm, width: 50–150 nm	Top-down	Biotin-avidin binding	Streptavidin	10 fM	Stern et al. (2007a), (2007b)
n-type poly-SiNW; width: 80 nm, lenght: 2 μm	Top-down	4-carboxyphenylboronic acid-dopamine interaction	Dopamine	1 fM	Lin et al. (2008)
n-type SiNW, p-type SiNW; thickness: 40 nm, width: 50–150 nm	Top-down	Antibody-antigen interaction	PSA, CA-15.3	PSA: 2.5 ng mL^{-1}, CA 15.3: 30 U/mL	Stern et al. (2010)
n-type SiNW; thickness: ≤40 nm	Top-down	Antibody-antigen interaction	PSA	30 aM	Kim et al. (2007)
n-type SiNW; width: 50 nm, thickness: 60 nm, length: 100 nm	Top-down	Antibody-antigen interaction	cTnT, Creatine kinase-MM and MB	1 pg/mL	Zhang et al. (2011b)
n-type SiNW; width: 50 nm, thickness: 60 nm, length: 100 nm	Top-down	Antibody-antigen interaction	cTnT	1 fg mL^{-1}	Chua et al. (2009)
n-type Polycrystalline (poly) Si NW	Top-down	Antibody-antigen interaction	PSA	5 fg/mL	Huang et al. (2013)
P-type SiNW; width: 60 nm, length: 10 μm	Top-down	Antibody-antigen interaction	Thyroid-Stimulating Hormone	0.11 pM	Lu et al. (2014)
n-type SiNW; width: 50 nm, thickness: 60 nm, length: 100 nm	Top-down	Protein-DNA interaction	Endoplasmic reticulum	10 fM	Zhang et al. (2011a)
n-type SiNW; width: 50 nm, thickness: 60 nm, length: 100 nm	Top-down	PNA-DNA hybridization	RT-PCR product of dengue serotype 2	10 fM	Zhang et al. (2010)
n-type SiNW; width: 50 nm, thickness: 60 nm, length: 100 nm	Top-down	PNA-DNA hybridization	microRNA	1 fM	Zhang et al. (2009)
n-type SiNW; width: 50 nm, thickness: 60 nm, length: 100 nm	Top-down	PNA-DNA hybridization	DNA	10 fM	Zhang et al. (2008a), (2008b)
n-type SiNW, p-type SiNW; width: 20 nm, length: 30 nm	Top-down	DNA-DNA hybridization	DNA	10 pM	Bunimovich et al. (2006)
n-type SiNW, p-type SiNW; width: 50 nm, length: 20 nm	Top-down	DNA-DNA hybridization	DNA	25 pM	Li et al., (2004, 2005)
p-type SiNW; width: 20 nm, heights: 30 nm	Top-down	DNA-DNA hybridization	DNA	10 fM	Nuzaihan et al. (2016)
p-type SiNW; width: 60 nm, heights: 200 nm	Top-down	DNA-DNA hybridization	DNA	1 nM	Pengfei et al. (2013)
p-type SiNW; width: 20 nm, heights: 1000 nm	Top-down	DNA-DNA hybridization	DNA	0.1 nM	Adam and Hashim (2014)
p-type SiNW; width: 50 nm, heights: 80 nm	Top-down	DNA-DNA hybridization	DNA	1 pM	Ryu et al. (2010)
p-type SiNW; width: 40 nm	Top-down	DNA-DNA hybridization	DNA	200 pM	Pham et al. (2011)
p-type SiNW; width: 20 nm	Top-down	DNA-DNA hybridization	DNA	1 fM	Gao et al. (2011)
p-type SiNW; length: 16 μm	Top-down	DNA-DNA hybridization	DNA	0.1 fM	Gao et al. (2012)

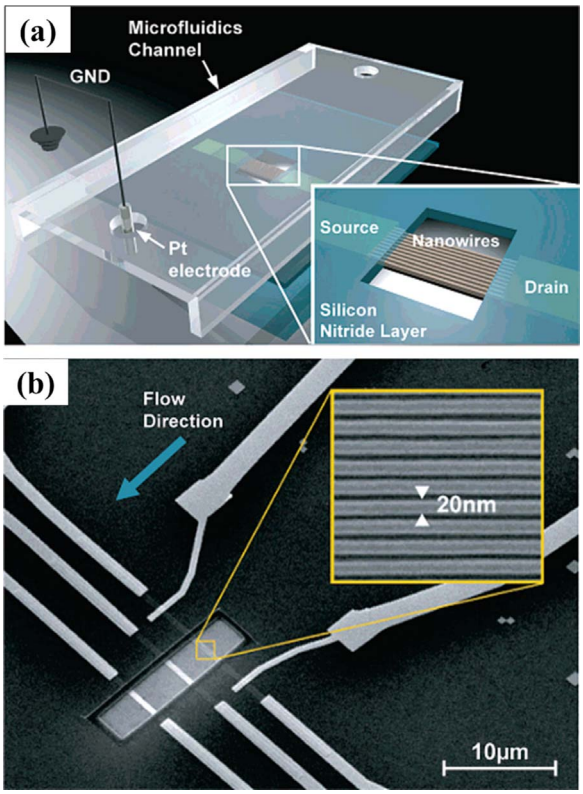

Fig. 4. Schematic diagram (a) and SEM image (b) of a single device section containing three groups of ~10 SiNWs in a microfluidics channel. Inset b is high-resolution SEM image of SiNWs. Images reprinted from (Bunimovich et al., 2006).

3.1.3. Titanium dioxide NWs-based FET biosensors

Titanium dioxide (TiO_2) has found applications in many promising areas due to their extraordinary large surface area, biocompatible, environmentally friendly, as well as unique chemical, physical, and electronic properties (Bai and Zhou, 2014). Chu et al. (2011) utilized monomer propylic acid to electropolymerize the polypyrrole propylic acid film on to the patterned TiO_2 NW surface for an abutment reaction. The initial step was agglutination of TiO_2 NW by using the hydrothermal method onto the exposed gated micro region. After electrochemical polymerization propylic acid with the antibody, the anti-rabbit immunoglobulin G was detected in the concentration range of 119 pg/mL to 5.95 ng/mL, the limits of detection was −3.96 A/(ng/mL) at the applied voltage of 5 V.

TiO_2 NWs are the ideal sensing material for FET based immunosensor, as they possess good chemical and photochemical stabilities, and have a negligible effect on protein denaturation. Wang and co-workers demonstrated the utilization of TiO_2 NW bundle microelectrode based FET immunosensor for sensitive, specific, and rapid detection of *L. monocytogenes* (Wang et al., 2008). This NW bundle based FET immunosensor detected as low as 10^2 cfu/mL of *L. monocytogenes* in 1 h without significant interference from other foodborne pathogens such as *E. coli* O157:H7, *S. Typhimurium*, and *S. aureus*. Recently, a conductance-based immunosensor was constructed based on an antibody/conducting polymer/TiO_2 NW by Lin et al. (2013). The fabricated devices detected 2 Ab within a linear range of 11.2 μg/mL to 112 μg/mL, with the detection sensitivity of −0.64 A/(g/mL). Recently, Guo et al. (2017) fabricated plasmon-enhanced biosensors to detect glucose and lactose. This cost-effective approach has potential to enhance sensing performance of NWs-based FET biosensors.

3.1.4. Gallium nitride NWs-based FET biosensors

Gallium nitride (GaN), a wide band-gap semiconductor has biological specificity for the variety of proteins and biomolecules, which are used to fabricate FET-based biosensors (Bain et al., 2013; Sahoo et al., 2013; Seo et al., 2015). Many groups demonstrated the use of AlGaN/GaN heterojunction FETs to detect biological target molecules such as DNAs and proteins with low concentrations (Jin et al., 2013; Lee et al., 2015a; Wen et al., 2011; Li et al., 2014). It has been recently shown that functionalization of GaN NWs may be of considerable interest for the development of high-performance semiconductor biomedical devices and as potential biosensing platforms for selective detection of proteins (Li et al., 2013). Williams et al. (2014) demonstrated a solution based functionalization method for the specific and selective attachment of streptavidin protein to GaN NWs. They performed all functionalization steps in solution, which enabled the assembly of multiple protein-specific NWs on a single biosensing platform. Streptavidin was immobilized on the 3-aminopropyltriethoxysilane (APTES) functionalized NWs. Such biotinylated GaN NW surface was highly specific towards the binding of streptavidin and demonstrated no affinity towards a control protein, bovine serum albumin (BSA). However, there was evidence of non-specific, electrostatic binding of both the streptavidin protein and the BSA protein to the APTES-coated NWs, revealing the importance of the biotinylation step. This study presented GaN NWs as a suitable material for protein sensing and for biosensing applications.

Chen et al. (2011a) demonstrated successful use of GaN-NW based an extended gate FET biosensor to detect human p53 tumor-suppressor gene. Pristine GaN was hydroxylated before immobilization of probe DNA varieties on the GaN surface. Then, the GaN surface was converted to (3-mercaptopropyl) trimethoxysilane and this surface exhibited the positive shift (I_D-V_{RE}) in the existence of negatively charged thiol groups. The (3-mercaptopropyl) trimethoxysilane modified GaN surface was incubated in the probe DNA solution to immobilize the DNA probe onto the surface. The simple sensor-architecture, by direct assembly of as-synthesized GaN NWs provided about a 6-orders lower detection limit with ~2 orders higher sensitivity over a wide detection range (10^{-19} to 10^{-6} M). The excellent specificity for target only in the presence of a complex system of foreign sequence reveals the potential of the biosensor device.

Simpkins et al. (2007) used both planer GaN substrates and individual GaN NWs to functionalize with ss-DNA. This study demonstrates successful immobilization of ss-DNA on GaN, in both planar and NW morphologies. Guo et al. (2010) reported an important strategy to increase surface immobilization in order to enhance the detection sensitivity of nanobiosensor. They utilized atomic layer deposition (ALD) to functionalize the GaN NW with Al_2O_3, SiO_2, and TiO_2. To attach streptavidin proteins on the GaN NWs, NWs were OH functionalized. The protein attachment was compared on the different surfaces, poly(ethylene glycol)-biotin, which was grafted on OH-functionalized GaN NW surfaces through active Si-Cl functional groups. Streptavidin protein molecules were then attached to the biotin ends. Among the three ALD coatings, ALD-SiO_2 yielded the most promising results in OH content and protein attachment. This study showed that ALD could be utilized for creating functional groups with much higher density compared to widely used acid modifications.

3.1.5. Indium oxide NWs-based FET biosensors

Indium oxide (In_2O_3) NWs is also potential nanomaterials for FET-based biosensing applications (Ishikawa et al., 2009a, 2009b). Chang et al. (2011) reported In_2O_3 NW FET-based label-free biosensing system that rapidly detected cancer biomarkers directly from human whole blood collected by a finger prick. As shown in the Fig. 6a, first, they collected blood through finger prick device, allowed to clot, and passed through the microfilter to remove blood cells. Fig. 6b shows the microscopic and optical images of a blood sample before and after filtration. The blood cells were almost completely filtered (99.6%), which was delivered to the nanosensor for electrical measurements (Fig. 6c). These nanosensors with In_2O_3 NWs were coated with the CA-125 antibody (Fig. 7a). The real-time response for CA-125 antibody coated device showed the decrease in S-D current and re-equilibrated to a

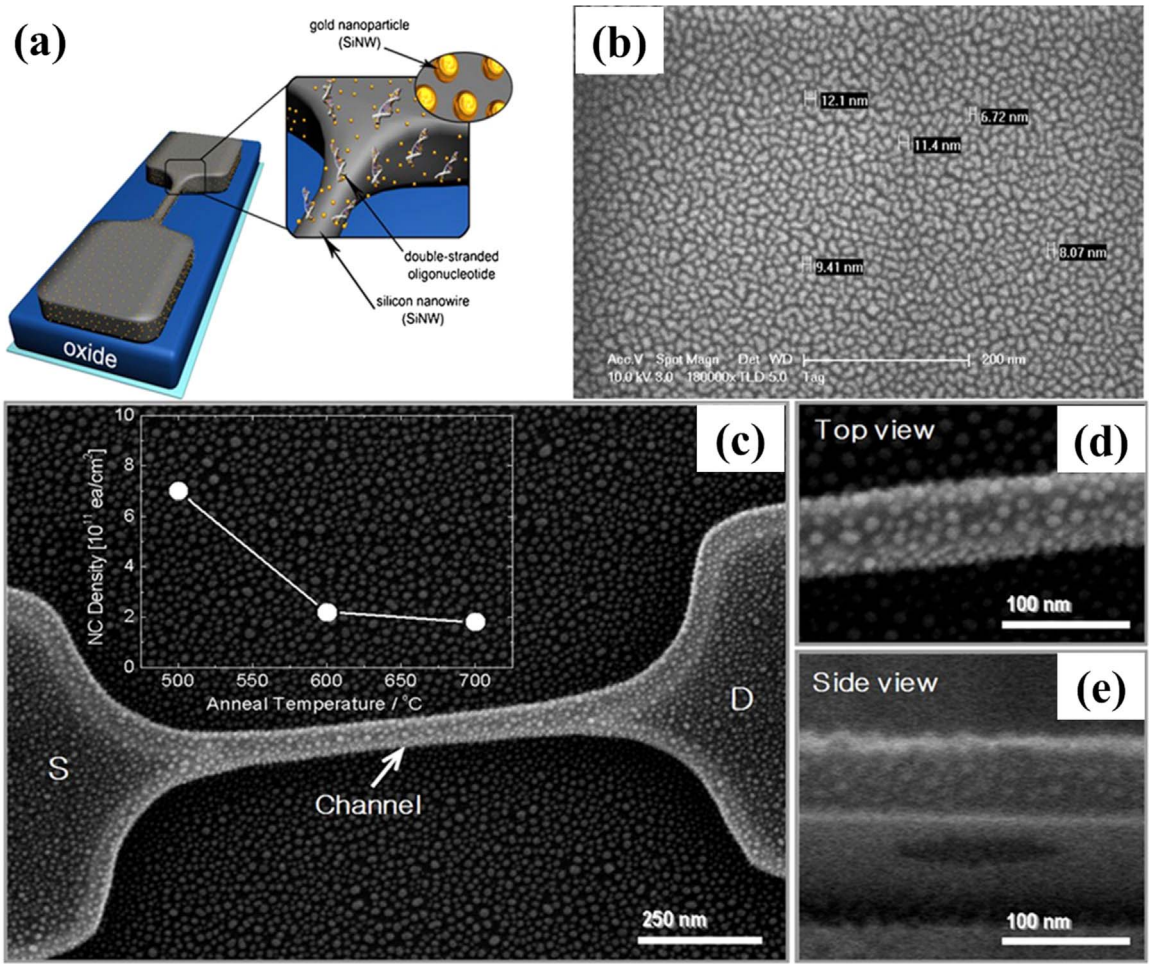

Fig. 5. (a) Schematic and (b-e) SEM images of the Au NPs embedded SiNW device. (b) The cracked Au film due to incomplete agglomeration at 400 °C and (c) Au NPs after complete agglomeration at 500 °C. The SEM high resolution view at the top (d) and the side (e) of the SiNW. Images reprinted from (Ryu et al., 2010).

lower level after being introduced to 1 U/mL CA-125 with the change in current about 1%. However, when the device was first submerged in serum and then exposed to CA-125 of 1 U/mL concentration, there was no noticeable sensing signal during real-time sensing response (Fig. 7b). Hence, the loss of sensing response in serum was due to the presence of nontargeted proteins in the serum that negatively impacts the sensitivity of nanosensors. Further, to overcome the limitation induced by nonspecific binding of nontargeted proteins, they utilized an amphipathic polymer, Tween 20, to passivated the NW surface that reduces nonspecific binding (Fig. 7c). The passivated device almost showed a similar response to the device in purified buffer (Fig. 7a), which clearly confirm that the Tween 20 passivation of NW surface protects the nonspecific binding of nontargeted proteins and retain the excellent sensing performance of fabricated devices even in the complex medium such as serum. Finally, devices were used to detect two epithelial ovarian cancer biomarkers, CA-125 and insulin-like growth factor II in real time. They got a 0.1 U/mL detection limit for CA-125 and an 8 ng/mL detection limit, which was at least 2 orders of magnitude lower than the clinically relevant level for diagnosis in both cases.

Ishikawa et al. (2009a) introduced, first time, application of antibody mimic proteins (AMPs) in the nanobiosensors field. AMPs are the polypeptides, which bind to their target analytes with high affinity and specificity, just like conventional antibodies, but are much smaller in size (2–5 nm, less than 10 kDa). They utilized In_2O_3 NWs to fabricate FET-based sensor after modifying with an AMP as a biomarker (Fibronectin, Fn), to detect a nucleocapsid protein biomarker associated with the severe acute respiratory syndrome coronavirus. BSA was used as passivation to get rid of nonspecific binding interactions of proteins with the NW device and probably false positive results (inset of Fig. 8c). Fig. 8a and b show the change of normalized current when adding BSA. After several times of BSA addition, the current stabilizes as a baseline and are suitable for the detection of N protein. The current response with the addition of different concentration of N protein is demonstrated in Fig. 8c. A higher concentration leads to a larger normalized current response. When Fn was removed, no significant response can be observed, confirming that the Fn-based capture probe can selectively capture the N protein. In another work, Ishikawa et al. (2009b) reported that the electrostatic interaction is the dominant sensing mechanism for In_2O_3 NW-based FET biosensors, and studied the correlation between the gate dependence and the absolute responses of biosensors measured by means of a liquid gated electrode. They developed a data analysis method to calibrate the sensor performance by dividing the absolute response by the gate dependence of each device and successfully reduced the device-to-device variation according to the correlation.

3.1.6. *Conducting polymer NWs-based FET biosensors*

Conducting polymer NWs, as a new member of one-dimensional nanostructured materials family has emerged as competitive sensing materials for biological sensing applications (Yang et al., 2014; Shrivastava et al., 2016; Meng et al., 2013). Their ease of synthesis by chemical or electrochemical techniques at ambient conditions, functionalization with monomer, dopant, monomer/dopant ratios and oxidation state to increase the conductivities over 15 orders of magnitude, biocompatibility, and low energy optical transitions have generated a great interest of researchers all over the world (Brooks and Sumerlin,

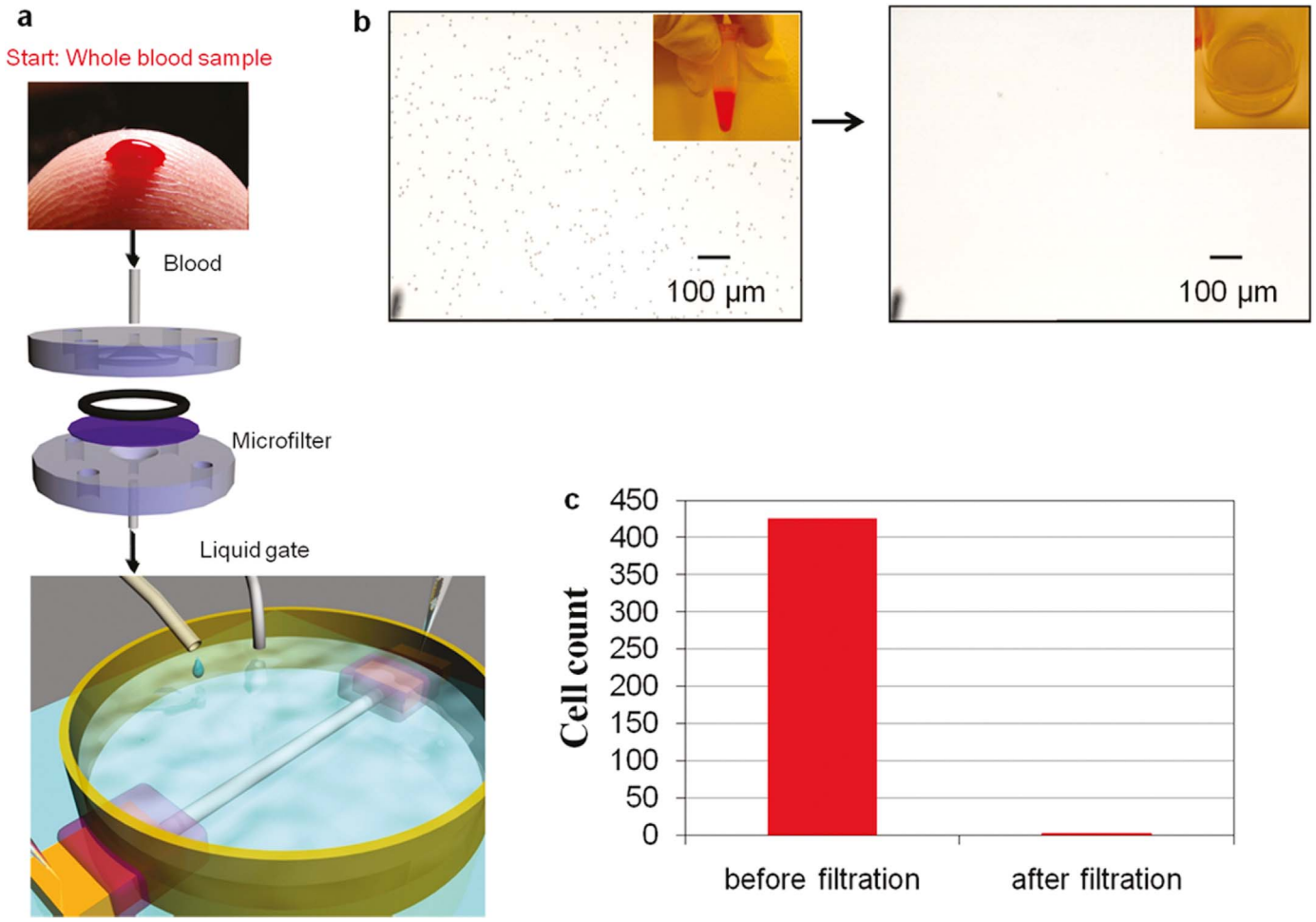

Fig. 6. (a) Schematic of nanobiosensor system, (b) microscopic and optical images (inset) image of blood sample and (c) cell count before and after microfiltration. Images reprinted from (Chang et al., 2012).

2016; Barsan et al., 2015; Kannan et al., 2012). Conducting polymers has been synthesized by different methods i.e. electrochemical dip-pen lithography, mechanical stretching, electrospinning and template-directed electrochemical synthesis (Yildiz et al., 2013; Mansour et al., 2016; Maziz et al., 2016). However, NWs of these conducting polymers (polypyrrole (PPy), polyaniline (PANI), poly(ethylene dioxythiophene) (PEDOT) and their functionalized derivatives) have been mostly used in biosensors applications (Travas-Sejdic et al., 2014).

Bangar et al. (2011) reported a highly sensitive, simple and label-free single PPy NW-based conductometric/chemiresistive DNA sensor. The fabricated FET sensor detected 19 base pair long breast cancer gene sequence with single nucleotide polymorphism discrimination with high sensitivity, a lower detection limit ($\sim 10^{-16}$ M) and wide dynamic range ($\sim 10^{-16}$ to 10^{-11} M) in a small sample volume (30 μL). The low detection limit ($\sim 10^{-16}$ M) was better than previous reports i.e. 10^{-9} M using avidin entrapped single conducting polymer based chemiresistive/FET sensor (Peng et al., 2009), 10^{-9} M using PEDOT nanotubules with physically entrapped probe ssDNA-based FET sensor (Krishnamoorthy et al., 2004), 10^{-9} M using poly(pyrrole-3-carboxylic acid) nanotubes-based FET sensor (Ko and Jang, 2008), 10^{-14} M using a PNA functionalized SiNW-FET sensor (Gao et al., 2007), and 10^{-13} M using Au NP enhanced DNA detection strategy utilizing carbon nanotube-based FET sensor (Dong et al., 2008). Further, DNA sensor also detected longer targets with 21 and 36 bases, which have implications in environmental sample analysis or metagenomics. Previously, Bangar et al. (2009) demonstrated the detection of cancer biomarker, cancer antigen 125 using glutaraldehyde and N-(3-dimethylaminopropyl)-N′-ethylcarbodiimide hydrochloride chemistries on a single PPy conducting polymer. The fabricated FET-based immunosensor had excellent sensitivity with a lower detection limit of 1 U/mL cancer antigen 125 and dynamic range up to 1000 U/mL. Also, sensor was checked in human blood plasma, which showed no loss of performance and great portability for diagnosis of patients at the point of care for cancer marker detection with cost benefits.

Ramanathan et al. (2004) demonstrated the use of single and multiple individually addressable controlled dimension, high aspect ratio (100 nm wide by up to 13 μm long) and dendrite-free NWs of conducting polymers PANI and PPy. They showed the ability to create scalable high density “arrays” by the site-specific positioning of conducting polymer NWs of same and different composition on the same chip. The change in resistance of PANI as a function of environment pH was evaluated, which showed a decrease in resistance by 4 orders of magnitude after addition of 0.1 M HCl. The resistance could be switched by 2–3 orders of magnitude by repeatedly cycling with water and 0.1 M HCl. A similar but lower resistance change was observed for PPy. The 4 order of magnitude resistance change observed. In another report, Ramanathan et al. (2005) utilized a similar approach to fabricated similar electrode structure with a channel 100 or 200 nm wide by 3 μm long was employed for the entrapment of the model protein, avidin, during electrochemical polymerization of PPy in a single step. Biotin conjugated to a 20-mer DNA oligo (biotin-DNA) was applied for sensor fabrication. The resistance of avidin-functionalized NWs was increased rapidly to a constant value upon addition of 1 nM of the biotin-DNA conjugate, and the resistance change increased with increasing

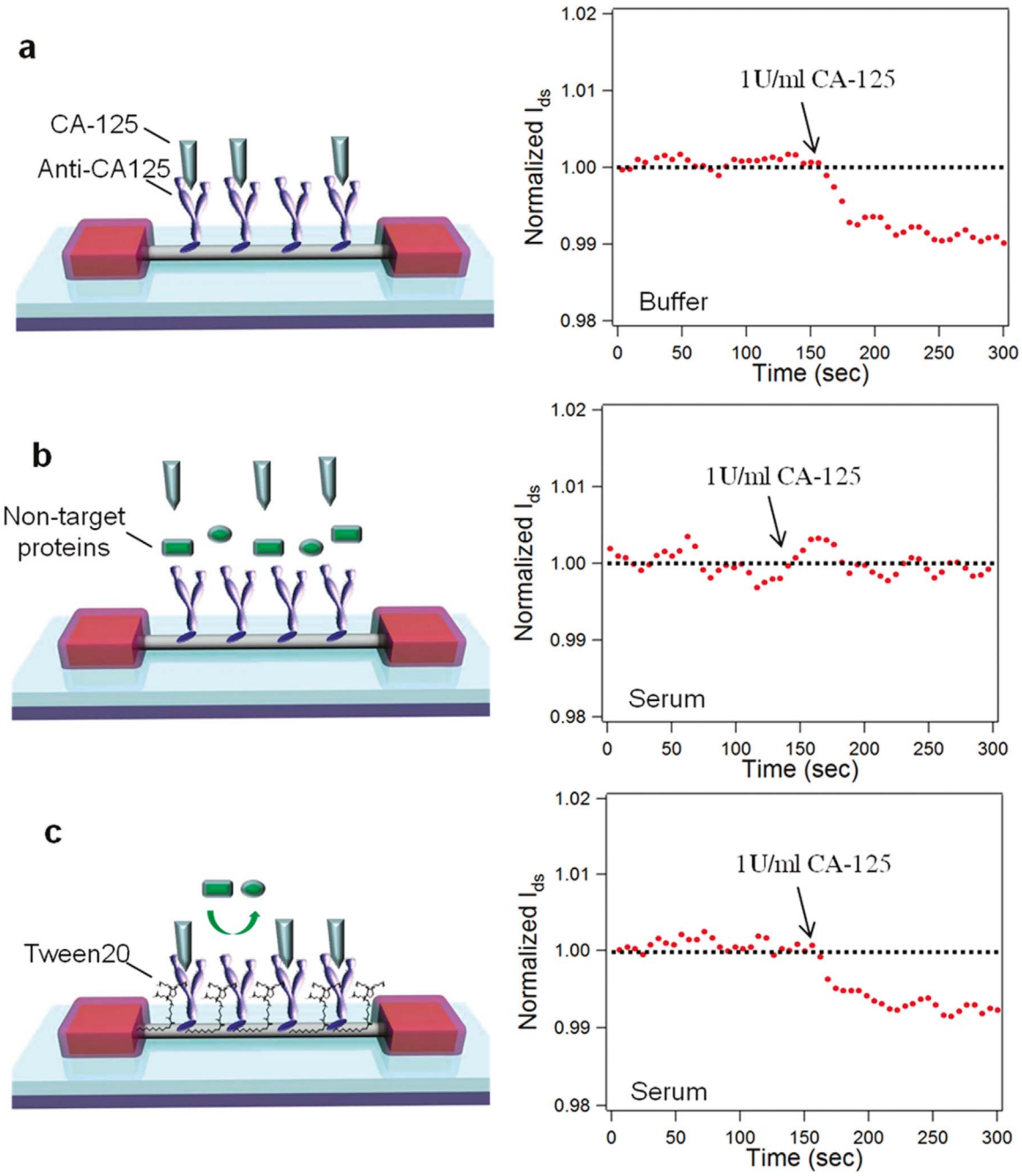

Fig. 7. Different device configurations and their real-time sensing response for (a) un-passivated CA-125 nanosensor in buffer, (b) un-passivated CA-125 nanosensor in serum, and (c) Tween 20-passivated nanosensor in serum. Images reprinted from (Chang et al., 2011).

concentrations up to 100 nM. Further increase in biotin-DNA conjugate concentration to 1 μM, resulted in only a 4% increase over 100 nM, indicating the saturation of recognition sites.

Uses of conducting polymers are not limited to nucleotide and biomarker detection. García-Aljaro et al. (2010) assembled PPy onto microfabricated Au interdigitated microelectrodes to construct a chemiresistive FET biosensor for the detection of *Bacillus globigii*. The fabricated FET biosensor showed excellent sensitivity with a detection limit of 1 cfu/mL and a dynamic range up to 100 cfu/mL. Shirale et al. (2010) reported fabrication of chemiresistive immunosensor FET based on single PPy NW for highly sensitive, specific, label free, and direct detection of viruses. The fabricated immunosensor showed lower detection limit of 10^{-3} plaque forming unit in 10 mM PBS, wide dynamic range and excellent selectivity. Also, sensors were applied to a real sample for phages detection, which shows the potential of these sensors in health care, environmental monitoring, food safety and homeland security for sensitive, specific, rapid, and affordable detection of bioagents/pathogens. Arter et al. (2012) demonstrated *de novo* fabrication of a biosensor based upon virus-containing PEDOT NWs, which detected prostate-specific membrane antigen (PSMA). When the fabricated device was introduced to PSMA in the concentration range of 20–120 nM in high ionic strength phosphate-buffered fluoride buffer, the electrical resistance of an array of these NWs was increased linearly, giving a very low LOD (56 nM) for PSMA.

4. Conclusions and future prospects

Unique and fascinating features of nanomaterials make them more

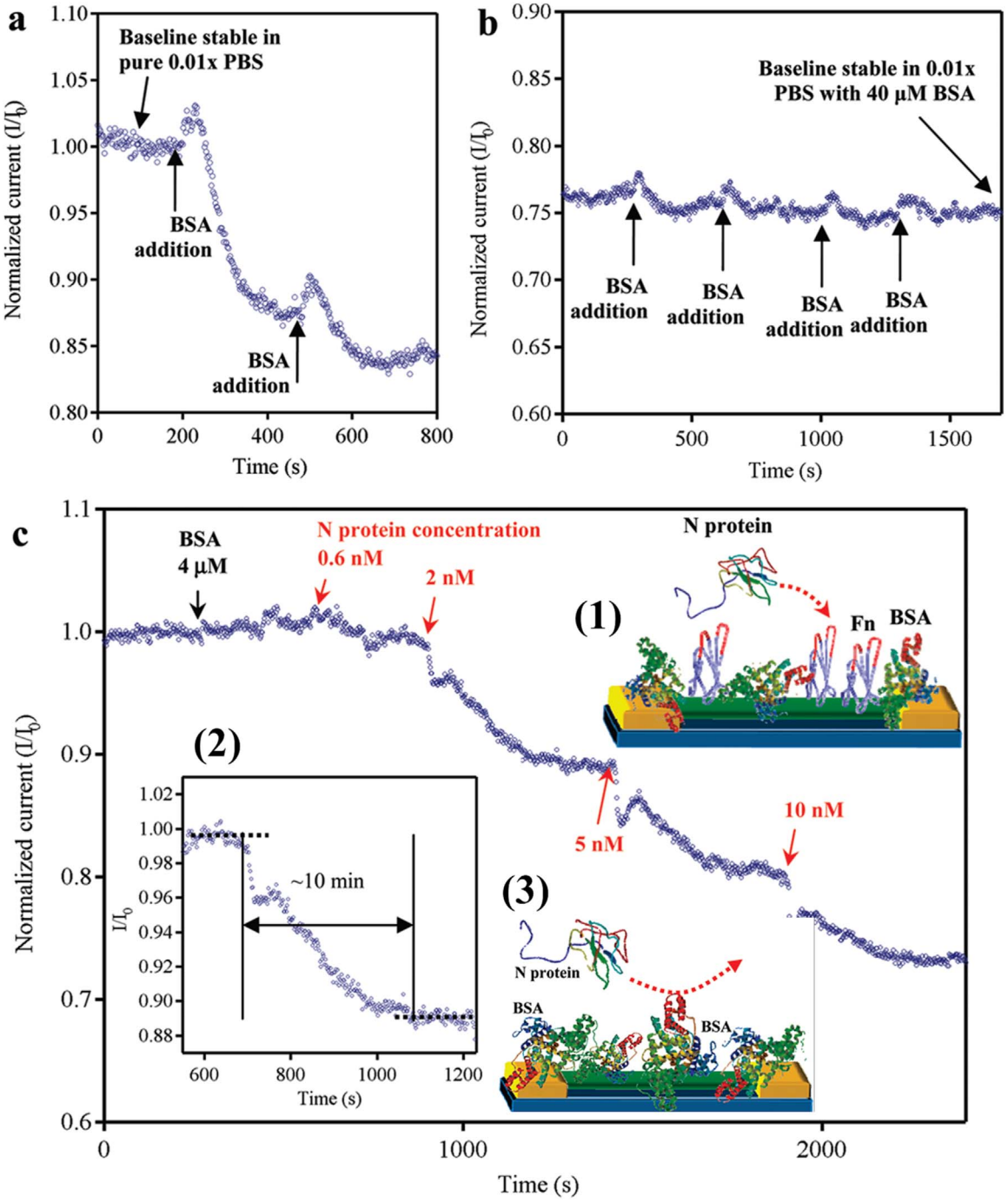

Fig. 8. Normalized electrical output (I/I_0) vs. time of a single operating device. (a-b) Response curves to passivation upon addition of successive aliquots of BSA. (c) Response for a nanowire device functionalized with Fn. Inset (1) is the device configuration during active sensing measurement. Inset (2) shows the plateau and the definition of response time. Inset (3) is schematic of a control device without Fn capture probe does not respond to the presence of N protein. Images reprinted from (Ishikawa et al., 2009a).

suitable than traditional materials. The high surface area and capability to be fabricated in many shapes and sizes has clearly enhanced the performances in terms of sensitivity and detection limits down to single molecules detection. Especially for the NWs-based biosensors fabrication, NWs not only improved the performance of biosensors but also reduced the size of the device, which enables detection of clinically important biomolecules in laboratories or at home. Furthermore, the combination/modification of different NWs with metal/metal oxide to increase even more the performances of biosensors is a well-accepted strategy. A vast number of different NWs-based biosensors all with its own specific properties have been recently published emphasizing the principal advantages of such NWs usages. However, the advantages of those novel biomolecular detection platforms over conventional bioassay tools remain to be clarified. Despite achieving high detection sensitivities by NWs-based biosensors, their reliability and reproducibility may need careful examinations. Also, as compared with other nano-biosensor systems, batch-to-batch variations in those NWs biosensors need more attention and may be minimized by further work.

In particular, NWs-based FETs biosensors have grown rapidly in last decade for application in electrical biosensing technology of medical diagnosis as well as electronic circuits. In biomedical diagnosis, they are applied as transducing component of biosensors. To target specific molecule, these biosensors are equipped with different immobilized bioreceptors probe (e.g., nucleic acids, antibodies, enzyme substrate).

Such biosensing devices are able to detect a wide range of molecular species with enhanced sensitivity and selectivity with applications in security, health care for point-of-care analyses of diseases, and environmental safety, which is of paramount importance for improving the quality of human life.

Despite remarkable progress in NWs-based FET biosensors, there are some major challenges to be addressed in future. The development of a reliable and scalable fabrication method is needed for the mass-production of identical NWs. Also, the integration of NWs into functional devices with high yields is another important issue. The fully integration of separation and purification processes are used to control NWs properties during device fabrication. Recently, solvent-based reproducible and controllable positioning, placement and orientation of NWs on the desired substrate locations are effectively utilized. From the application point of view, the development of a simple and reliable reference electrode integration method and diagnosis under physiological conditions may lead to a new generation of devices. Additionally, fouling during bioanalytical applications in a real sample is another problem, which greatly reduces the sensitivity of the device during detection of specific targets. To overcome this issue, antifouling surface coatings are mainly used to reduce/minimize nonspecific interactions. Moreover, introduction of microfluidics to the devices for designing lab-on-a-chip based nanosensor devices will strongly benefit the miniaturization, nano-fabrication, and combining the stereo specificity of biological macromolecules, to get the desired result of ultra-sensitive micro sized diagnostics, within the reach of patient, physician, emergency room, hospital use in static and dynamic continuous monitoring mode.

Acknowledgements

This work was supported by the National Leading Research Laboratory program through the National Research Foundation (NRF) (NRF-2016R1A2B2016665) of Korea funded by the Ministry of Science, ICT & Future Planning.

References

Adam, T., Hashim, U., 2014. Biosens. Bioelectron. 7184, 1.
Ahmad, R., Tripathy, N., Hahn, Y.-B., 2013. Biosens. Bioelectron. 45, 281.
Ahmad, R., Tripathy, N., Park, J.-H., Hahn, Y.-B., 2015. Chem. Commun. 51, 11968.
Ahmad, R., Ahn, M.-S., Hahn, Y.-B., 2017a. Electrochem. Commun. 77, 107.
Ahmad, R., Tripathy, N., Ahn, M.-S., Bhat, K.S., Mahmoudi, T., Wang, Y., Yoo, J.-Y., Kwon, D.-W., Yang, H.-Y., Hahn, Y.-B., 2017b. Sci. Rep. 7, 5715.
Ahmad, R., Tripathy, N., Ahn, M.-S., Hahn, Y.-B., 2017c. Sci. Rep. 7, 46475.
Arter, J.A., Diaz, J.E., Donavan, K.C., Yuan, T., Penner, R.M., Weiss, G.A., 2012. Anal. Chem. 84, 2776.
Artiles, M.S., Rout, C.S., Fisher, T.S., 2011. Adv. Drug Deliv. Rev. 63, 1352.
Arya, S.K., Wong, C.C., Jeon, Y.J., Bansal, T., Park, M.K., 2015. Chem. Rev. 115, 5116.
Asif, M.H., Nur, O., Willander, M., Danielsson, B., 2009. Biosens. Bioelectron. 24, 3379.
Ashley, J., Shahbazi, M.-A., Kant, K., Chidambara, V.A., Wolff, A., Bang, D.D., Sun, Y., 2017. Biosens. Bioelectron. 91, 606.
Bai, J., Zhou, B., 2014. Chem. Rev. 114, 10131.
Bain, L.E., Jewett, S.A., Mukund, A.H., Bedair, S.M., Paskova, T.M., Ivanisevic, A., 2013. ACS Appl. Mater. Interfaces 5, 7236.
Balasubramanian, K., 2010. Biosens. Bioelectron. 26, 1195.
Bangar, M.A., Shirale, D.J., Chen, W., Myung, N.V., Mulchandani, A., 2009. Anal. Chem. 81, 2168.
Bangar, M.A., Shirale, D.J., Purohit, H.J., Chen, W., Myung, N.V., Mulchandani, A., 2011. Electroanalysis 23, 371.
Barsan, M.M., Ghica, M.E., Brett, C.M.A., 2015. Anal. Chim. Acta 881, 1.
Bergveld, P., 1970. IEEE Trans. Biomed. Eng. 17, 70.
Brooks, W.L.A., Sumerlin, B.S., 2016. Chem. Rev. 116, 1375.
Bunimovich, Y.L., Shin, Y.S., Yeo, W.-S., Amori, M., Kwong, G., Heath, J.R., 2006. J. Am. Chem. Soc. 128, 16323.
Cella, L.N., Chen, W., Myung, N.V., Mulchandani, A., 2010. J. Am. Chem. Soc. 132, 5024.
Citartan, M., Gopinath, S.C., Tominaga, J., Tang, T.H., 2013. Analyst 138, 3576.
Chang, H.-K., Ishikawa, F.N., Zhang, R., Datar, R., Cote, R.J., Thompson, M.E., Zhou, C., 2011. ACS Nano 5, 9883.
Chen, C.-P., Ganguly, A., Lu, C.-Y., Chen, T.-Y., Kuo, C.-C., Chen, R.-S., Tu, W.-H., Fischer, W.B., Chen, K.-H., Chen, L.-C., 2011a. Anal. Chem. 83, 1938.
Chen, K.-I., Li, B.-R., Chen, Y.-T., 2011b. Nano Today 6, 131.
Chen, T.-Y., Loan, P.T.K., Hsu, C.-L., Lee, Y.-H., Wang, J.T.-W., Wei, K.-H., Lin, C.-T., Li, L.-J., 2013. Biosens. Bioelectron. 41, 103.
Cheran, L.-E., Cheran, A., Thompson, M., 2014. Chapter 1: Biomimicry Mater. Med. Adv. Synth. Mater. Detect. Sci. 2014, 1.
Choi, A., Kim, K., Jung, H.-I., Lee, S.Y., 2010. Sens. Actuator B-Chem. 148, 577.
Chu, Y.M., Lin, C.C., Chang, H.C., Li, C., Guo, C., 2011. Biosens. Bioelectron. 26, 2334.
Chua, J., Chee, R.E., Agarwal, A., Wong, S.M., Zhang, G.-J., 2009. Anal. Chem. 81, 6266.
Cui, Y., Wei, Q.Q., Park, H.K., Lieber, C.M., 2001. Science 293, 1289.
Dong, X., Lau, C.M., Lohani, A., Mhaisalkar, S.G., Kasim, J., Shen, Z., Ho, X., Rogers, J.A., Li, L.-J., 2008. Adv. Mater. 20, 2389.
Drobek, M., Kim, J.-H., Bechelany, M., Vallicari, C., Julbe, A., Kim, S.S., 2016. ACS Appl. Mater. Interfaces 8, 8323.
Du, X., Li, Y., Motley, J.R., Stickle, W.F., Herman, G.S., 2016. ACS Appl. Mater. Interfaces 8, 7631.
Feigel, I.M., Vedala, H., Star, A., 2011. J. Mater. Chem. 21, 8940.
Gao, A., Lu, N., Dai, P., Li, T., Pei, H., Gao, X., Gong, Y., Wang, Y., Fan, C., 2011. Nano Lett. 11, 3974.
Gao, A., Lu, N., Wang, Y., Dai, P., Li, T., Gao, X., Wang, Y., Fan, C., 2012. Nano Lett. 12, 5262.
Gao, X.P.A., Zheng, G., Lieber, C.M., 2010. Nano Lett. 10, 547.
Gao, Z.Q., Agarwal, A., Trigg, A.D., Singh, N., Fang, C., Tung, C.H., Fan, Y., Buddharaju, K.D., Kong, J.M., 2007. Anal. Chem. 79, 3291.
García-Aljaro, C., Bangar, M.A., Baldrich, E., Munoz, F.J., Mulchandani, A., 2010. Biosens. Bioelectron. 25, 2309.
Guo, D.J., Abdulagatov, A.I., Rourke, D.M., Bertness, K.A., George, S.M., Lee, Y.C., Tan, W., 2010. Langmuir 26, 18382.
Guo, L., Li, Z., Marcus, K., Navarro, Liang, S.K., Zhou, L., Mani, P.D., Florczyk, S.J., Coffey, K.R., Orlovskaya, N., Sohn, Y.-H., Yang, Y., 2017. ACS Sens. 2, 621.
Hahm, J.-I., Lieber, C.M., 2004. Nano Lett. 4, 51.
Hahn, Y.B., 2011. Korean J. Chem. Eng. 28, 1797.
Han, D., Chand, R., Kim, Y.-S., 2017. Biosens. Bioelectron. 93, 220.
Heller, A., Feldman, B., 2008. Chem. Rev. 108, 2482.
Hobbs, R.G., Petkov, N., Holmes, J.D., 2012. Chem. Mater. 24, 1975.
Huang, C., Notten, A., Rasters, N., 2011a. J. Technol. Transf. 36, 145.
Huang, W., Diallo, A.K., Dailey, J.L., Besar, K., Katz, H.E., 2015. J. Mater. Chem. C 3, 6445.
Huang, Y., Dong, X., Liu, Y., Li, L.-J., Chen, P., 2011b. J. Mater. Chem. 21, 12358.
Huang, Y., Dong, X., Shi, Y., Li, C.M., Li, L.-J., Chen, P., 2010. Nanoscale 2, 1485.
Huang, Y.-W., Wu, C.-S., Chuang, C.-K., Pang, S.-T., Pan, T.-M., Yang, Y.-S., Ko, F.-H., 2013. Anal. Chem. 85, 7912.
Ishikawa, F.N., Chang, H.-K., Curreli, M., Liao, H.-I., Olson, C.A., Chen, P.-C., Zhang, R., Roberts, R.W., Sun, R., Cote, R.J., Thompson, M.E., Zhou, C., 2009a. ACS Nano 3, 1219.
Ishikawa, F.N., Curreli, M., Chang, H.K., Chen, P.C., Zhang, R., Cote, R.J., Thompson, M.E., Zhou, C.W., 2009b. ACS Nano 3, 3969.
Jiang, H., 2011. Small 7, 2413.
Jin, H.-E., Zueger, C., Chung, W.-J., Wong, W., Lee, B.Y., Lee, S.-W., 2015. Nano Lett. 15, 7697.
Jin, W.X., Nian, W.S., Ji, W.Y., James, L.L., Wu, L., 2013. Chin. Sci. Bull. 58, 2601.
Kaisti, M., 2017. Biosens. Bioelectron. 98, 437.
Kannan, B., Williams, D.E., Laslau, C., Travas-Sejdic, J., 2012. Biosens. Bioelectron. 35, 258.
Keem, K., Jeong, D.Y., Kim, S., Lee, M.S., Yeo, I.S., Chung, U.I., Moon, J.T., 2007. Nano Lett. 6, 1454.
Kergoat, L., Piro, B., Berggren, M., Horowitz, G., Pham, M.-C., 2012. Anal. Bioanal. Chem. 402, 1813.
Kim, A., Ah, C.S., Yu, H.Y., Yang, J.H., Baek, I.B., Ahn, C.G., Park, C.W., Jun, M.S., Lee, S., 2007. Appl. Phys. Lett. 91, 103901.
Kim, S.G., Lee, J.S., Jun, J., Shin, D.H., Jang, J., 2016. ACS Appl. Mater. Interfaces 8, 6602.
Ko, S., Jang, J., 2008. Ultramicroscopy 108, 1328.
Krishnamoorthy, K., Gokhale, R.S., Contractor, A.Q., Kumar, A., 2004. Chem. Commun. 7, 820.
Lee, H.H., Bae, M., Jo, S.-H., Shin, J.-K., Son, D.H., Won, C.-H., Jeong, H.-M., Lee, J.-H., Kang, S.-W., 2015a. Sensors 15, 18416.
Lee, J., Jang, J., Choi, B., Yoon, J., Kim, J.-Y., Choi, Y.-K., Kim, D.M., Kim, D.H., Choi, S.-J., 2015b. Sci. Rep. 5, 12286.
Li, J.-d., Cheng, J.-j., Miao, B., Wei, X.-W., Xie, J., Zhang, J.-C., Zhang, Z.-Q., Wu, D.-M., 2014. J. Micromech. Microeng. 24, 075023.
Li, J., Han, Q., Zhang, Y., Zhang, W., Dong, M., Besenbacher, F., Yang, R., Wang, C., 2013. ACS Appl. Mater. Interfaces 5, 9816.
Li, Z., Chen, Y., Li, X., Kamins, T.I., Nauka, K., Williams, R.S., 2004. Nano Lett. 4, 245.
Li, Z., Rajendran, B., Kamins, T.I., Li, X., Chen, Y., Williams, R.S., 2005. Appl. Phys. A 80, 1257.
Lin, C.-C., Chu, Y.-M., Chang, H.-C., 2013. Sens. Actuators B 187, 533.
Lin, C.-H., Hsiao, C.-Y., Hung, C.-H., Lo, Y.-R., Lee, C.-C., Su, C.-J., Lin, H.-C., Ko, F.-H., Huang, T.-Y., Yang, Y.-S., 2008. Chem. Commun. 5749.
Lin, T.W., Hsieh, P.J., Lin, C.L., Fang, Y.Y., Yang, J.X., Tsai, C.C., Chiang, P.L., Pan, C.Y., Chen, Y.T., 2010. Proc. Natl. Acad. Sci. USA 107, 1047.
Liu, S., Guo, X., 2012. NPG Asia Mater. 4, 23.
Liu, X., Lina, P., Yan, X., Kang, Z., Zhao, Y., Lei, Y., Li, C., Du, H., Zhang, Y., 2013. Sens. Actuator B-Chem. 176, 22.
Lu, N., Dai, P., Gao, A., Valiaho, J., Kallio, P., Wang, Y., Li, T., 2014. ACS Appl. Mater. Interfaces 6, 20378.
Luong, J.H.T., Vashist, S.K., 2017. Biosens. Bioelectron. 89, 293.
Maehashi, K., Sofue, Y., Okamoto, S., Ohno, Y., Inoue, K., Matsumoto, K., 2013. Sens. Actuator B-Chem. 187, 45.
Majd, S.M., Salimi, A., Astinchap, B., 2017. Biosens. Bioelectron. 92, 733.
Mao, Y., Shin, K.-S., Wang, X., Ji, Z., Meng, H., Chui, C.O., 2016. Sci. Rep. 6, 24982.

Mansour, N., Hriz, K., Jaballah, N., Kreher, D., Majdoub, M., 2016. Opt. Mater. 58, 296.
Maziz, A., Plesse, C., Soyer, C., Cattan, E., Vidal, F., 2016. ACS Appl. Mater. Interfaces 8, 1559.
Meng, F., Shi, W., Sun, Y., Zhu, X., Wu, G., Ruan, C., Liu, X., Ge, D., 2013. Biosens. Bioelectron. 42, 141.
Minami, T., Sasaki, Y., Minamiki, T., Wakida, S.-I., Kurita, R., Niwa, O., Tokito, S., 2016. Biosens. Bioelectron. 81, 87.
Monopoli, M.P., Åberg, C., Salvati, A., Dawson, K.A., 2012. Nat. Nanotechnol. 7, 779.
Nair, P., Alam, M., 2007. IEEE Trans. Electron Dev. 54, 3400.
Namdari, P., Daraee, H., Eatemadi, A., 2016. Nanoscale Res. Lett. 11, 406.
Nuzaihan, M.N., M., Hashim, U., Arshad, M.K.M., Ruslinda, A.R., Rahman, S.F.A., Fathil, M.F.M., Ismail, M.H., 2016. PLoS ONE 11, e0152318.
Park, M.-H., Han, D., Chand, R., Lee, D.-H., Kim, Y.-S., 2016. J. Phys. Chem. C 120, 4854.
Patolsky, F., Zheng, G., Hayden, O., Lakadamyali, M., Zhuang, X., Lieber, C.M., 2004. Proc. Natl. Acad. Sci. USA 101, 14017.
Peng, N., Zhang, Q., Chow, C.L., Tan, O.K., Marzari, N., 2009. Nano Lett. 9, 1626.
Pengfei, D., Anran, G., Na, L., Tie, L., Yuelin, W., 2013. Jpn. J. Appl. Phys. 52, 121301.
Piccinini, E., Bliem, C., Reiner-Rozman, C., Battaglini, F., Azzaroni, O., Knoll, W., 2017. Biosens. Bioelectron. 92, 661.
Pham, V.B., Pham, X.T.T., Dang, N.T.D., Le, T.T.T., Tran, P.D., Nguyen, T.C., Nguyen, V.Q., Dang, M.C., Rijn, C.J.M.V., Tong, D.H., 2011. Adv. Nat. Sci.: Nanosci. Nanotechnol. 2, 025010.
Puchnin, K., Andrianova, M., Kuznetsov, A., Kovalev, V., 2017. Biosens. Bioelectron. 98, 140.
Puppo, F., Doucey, M.-A., Delaloye, J.-F., Moh, T.S.Y., Pandraud, G., Sarro, P.M., Micheli, G.D., Carrara, S., 2014. IEEE Sens 866.
Ra, H.W., Choi, D.H., Kim, S.H., Im, Y.H., 2009. J. Phys. Chem. C 113, 3512.
Ra, H.-W., Kim, J.-T., Khan, R., Sharma, D., Yook, Y.-G., Hahn, Y.-B., Park, J.-H., Kim, D.-G., Im, Y.-H., 2012. Nano Lett. 12, 1891.
Ramanathan, K., Bangar, M.A., Yun, M., Chen, W., Mulchandani, A., Myung, N.V., 2004. Nano Lett. 4, 1237.
Ramanathan, K., Bangar, M.A., Yun, M., Chen, W., Myung, N.V., Mulchandani, A., 2005. J. Am. Chem. Soc. 127, 496.
Rashid, J.I.A., Abdullah, J., Yusof, N.A., Hajian, R., 2013. J. Nanomater. 2013, 328093.
Rees, F., Hui, M., Doherty, M., 2014. Nat. Rev. Rheumatol. 10, 271.
Regonda, S., Tian, R., Gao, J., Greene, S., Ding, J., Hu, W., 2013. Biosens. Bioelectron. 45, 245.
Rubtsova, M., Presnova, Presnov, G.D., Krupenin, V., Egorov, A., 2017. Procedia Technol. 27, 234.
Ryu, S.-W., Kim, C.-H., Han, J.-W., Kim, C.-J., Jung, C., Park, H.G., Choi, Y.-K., 2010. Biosens. Bioelectron. 25, 2182.
Sadeghian, R.B., Han, J., Ostrovidov, S., Salehi, S., Bahraminejad, B., Ahadian, S., Chen, M., Khademhosseini, A., 2017. Biosens. Bioelectron. 88, 41.
Sahoo, P., Suresh, S., Dhara, S., Saini, G., Rangarajan, S., Tyagi, A.K., 2013. Biosens. Bioelectron. 44, 164.
Sang, S., Wang, Y., Feng, Q., Wei, Y., Ji, J., Zhang, W., 2015. Crit. Rev. Biotechnol. 15, 1.
Sarkar, D., Liu, W., Xie, X., Anselmo, A.C., Mitragotri, S., Banerjee, K., 2014. ACS Nano 8, 3992.
Seo, T.H., Park, A.H., Park, S., Kim, Y.H., Lee, G.H., Kim, M.J., Jeong, M.S., Lee, Y.H., Hahn, Y.-B., Suh, E.-K., 2015. Sci. Rep. 5, 7747.
Simpkins, B.S., McCoy, K.M., Whitman, L.J., Pehrsson, P.E., 2007. Nanotechnol 18, 355301.
Sinha, M., Mahapatra, R., Mondal, B., Maruyama, T., Ghosh, R., 2016. J. Phys. Chem. C 120, 3019.
Shavanova, K., Bakakina, Y., Burkova, I., Shtepliuk, I., Viter, R., Ubelis, A., Beni, V., Starodub, N., Yakimova, R., Khranovskyy, V., 2016. Sensors 16, 223.
Shen, G.-H., Tandioa, A.R., Hong, F.C.-N., 2016. Thin Solid Films 618 (Part A), 100.
Shirale, D.J., Bangar, M.A., Park, M., Yates, M.V., Chen, W., Myung, N.V., Mulchandani, A., 2010. Environ. Sci. Technol. 44, 9030.
Shoorideh, K., Chui, C.O., 2014. PNAS 11, 5111.
Shrestha, B.K., Ahmad, R., Shrestha, S., Park, C.H., Kim, C.S., 2017. Biosens. Bioelectron. 94, 686.
Shrivastava, S., Jadon, N., Jain, R., 2016. TrAC Trends Anal. Chem. 82, 55.
Stern, E., Klemic, J.F., Routenberg, D.A., Wyremebak, P.N., Turner-Evans, D.B., Hamilton, A.D., LaVan, D.A., Fahmy, T.M., Reed, M.A., 2007a. Nature 445, 519.
Stern, E., Wagner, R., Sigworth, F.J., Breaker, R., Fahmy, T.M., Reed, M.A., 2007b. Nano Lett. 7, 3405.
Stern, E., Vacic, A., Rajan, N.K., Criscione, J.M., Park, J., Ilic, B.R., Mooney, D.J., Reed, M.A., Fahmy, T.M., 2010. Nat. Nanotechnol. 5, 138.
Sudibya, H.G., He, Q., Zhang, H., Chen, P., 2011. ACS Nano 5, 1990.
Tan, F., Saucedo, N.M., Ramnani, P., Mulchandani, A., 2015. Environ. Sci. Technol. 49, 9256.
Tran, D.P., Winter, M.A., Wolfrum, B., Stockmann, R., Yang, C.-T., Pourhassan-Moghaddam, M., Offenhäusser, A., Thierry, B., 2016. ACS Nano 10, 2357.
Travas-Sejdic, J., Aydemir, N., Kannan, B., Williams, D.E., Malmström, J., 2014. J. Mater. Chem. B 2, 4593.
Turner, A.P., 2013. Chem. Soc. Rev. 42, 3184.
Verma, V.P., Jeon, H., Hwang, S., Jeon, M., Choi, W., 2008. IEEE Trans. Nanotechnol. Adv. 7, 782.
Vigneshvar, S., Sudhakumari, C.C., Senthilkumaran, B., Prakash, H., 2016. Front. Bioeng. Biotechnol. 4, 11.
Wang, L., Wang, Y., Wong, J.I., Palacios, T., Kong, J., Yang, H.Y., 2014. Small 10, 1101.
Wang, R., Ruan, C., Kanayeva, D., Lassiter, K., Li, Y., 2008. Nano Lett. 8, 2625.
Wang, Z., Tian, Z., Han, D., Gu, F., 2016. ACS Appl. Mater. Interfaces 8, 5466.
Weintraub, A.S., Blanco, V., Barnes, M., Green, R.S., 2015. J. Perinatol. 35, 52.
Wen, X., Gupta, S., Wang, Y., Nicholson III, T.R., Lee, S.C., Lu, W., 2011. Appl. Phys. Lett. 99, 043701.
Williams, E.H., Davydov, A.V., Oleshko, V.P., Steffens, K.L., Levin, I., Lin, N.J., Bertness, K.A., Manocchi, A.K., Schreifels, J.A., Rao, M.V., 2014. Surf. Sci. 627, 23.
Yang, F., Zhang, G.-J., 2014. Rev. Anal. Chem. 33, 95.
Yang, N., Chen, X., Ren, T., Zhang, P., Yang, D., 2015. Sens. Actuator B-Chem. 207, 690.
Yang, T., Meng, L., Zhao, J., Wang, X., Jiao, K., 2014. ACS Appl. Mater. Interfaces 6, 19050.
Ye, D.-X., Ma, Y.-Y., Zhao, W., Cao, H.-M., Kong, J.-L., Xiong, H.-M., Möhwald, H., 2016. ACS Nano 10, 4294.
Yildiz, H.B., Caliskan, S., Kamaci, M., Caliskan, A., Yilmaz, H., 2013. Int. J. Biol. Macromol. 56, 34.
Yu, R., Pan, C., Chen, J., Zhu, G., Wang, Z.L., 2013. Adv. Funct. Mater. 23, 5868.
Zhang, C., Xu, J.-Q., Li, Y.-T., Huang, L., Pang, D.-W., Ning, Y., Huang, W.-H., Zhang, Z., Zhang, G.-J., 2016. Anal. Chem. 88, 4048.
Zhang, G.-J., Zhang, G., Chua, J.H., Chee, R.E., Wong, E.H., Agarwal, A., Buddharaju, K.D., Singh, N., Gao, Z.Q., Balasubramanian, N., 2008a. Nano Lett. 8, 1066.
Zhang, G.-J., Chua, J.H., Chee, R.E., Agarwal, A., Wong, S.M., Buddharaju, K.D., Balasubramanian, N., 2008b. Biosens. Bioelectron. 23, 1701.
Zhang, G.-J., Chua, J.H., Chee, R.E., Agarwal, A., Wong, S.M., 2009. Biosens. Bioelectron. 24, 2504.
Zhang, G.-J., Zhang, L., Huang, M.J., Luo, Z.H.H., Tay, G.K., Lim, E.-J., Kang, T.G., Chen, Y., 2010. Sens. Actuator B-Chem. 146, 138.
Zhang, G.-J., Huang, M., Ang, J., Liu, E.T., Desai, K.V., 2011a. Biosens. Bioelectron. 26, 3233.
Zhang, G.-J., Luo, Z.H.H., Huang, M.J., Ang, J.A.J., Kang, T.G., Ji, H.M., 2011b. Biosens. Bioelectron. 28, 459.
Zhang, G.-J., Ning, Y., 2012. Anal. Chim. Acta 749, 1.
Zheng, C., Huang, L., Zhang, H., Sun, Z., Zhang, Z., Zhang, G.-J., 2015. ACS Appl. Mater. Interfaces 7, 16953.
Zheng, G., Patolsky, F., Cui, Y., Wang, W.U., Lieber, C.M., 2005. Nat. Biotechnol. 23, 1294.